Rotational Dynamics of the Epidermal Growth Factor Receptor†

Richard A. Stein,‡ Eric J. Hustedt,§ James V. Staros,*,‡ and Albert H. Beth*,§

Department of Biological Sciences and Department of Molecular Physiology and Biophysics, Vanderbilt University, Nashville, Tennessee 37235

Received August 30, 2001; Revised Manuscript Received November 15, 2001

ABSTRACT: We have examined the rotational mobility of SL-EGF, a bifunctional adduct of bis(sulfo-*N*-succinimidyl)-[^{15}N,^{2}H$_{16}$]-doxyl-2-*spiro*-4′-pimelate and [Lys3,Tyr22]-murine epidermal growth factor, bound to the EGF receptor in A431 membrane vesicles. The linear EPR spectrum indicated that there was essentially no free SL-EGF in the bound complex preparation. To better define the rotational mobility of the SL-EGF bound to the EGF receptor, ST-EPR spectra were obtained at multiple Zeeman field modulation frequencies. Global analysis with a uniaxial rotational diffusion model of the ST-EPR data yielded two minima that have differences in rotational mobility and in orientation of the SL-EGF relative to the membrane normal axis. The rotational mobilities of the two rotational species are consistent with monomers and dimers or somewhat larger oligomers, such as trimers or tetramers, arguing against a role for higher order receptor clustering in receptor activation. Considering the two minima and previous observations that A431 membrane vesicles contain two distinguishable ligand-binding populations, the ST-EPR spectra were fit with a model having two uniaxial rotating species. This yielded two components that were similar to those obtained from the two original one-component fits, either fast or slow rotational mobility, with different orientations. The model-dependent results obtained suggest that there are potential conformational and rotational differences in the two populations and provide a plausible description for the origin of high- and low-affinity EGF-binding sites that can be tested in future experiments.

Epidermal growth factor (EGF), a 53 amino acid mitogenic polypeptide hormone, upon binding to its plasma membrane receptor activates the cytoplasmic protein tyrosine kinase domain of the receptor (*1*−*5*). Activation of the protein tyrosine kinase activity of the receptor results in an increase in autophosphorylation of its carboxyl-terminal region and an increase in phosphorylation of other cellular proteins. The subsequent cascade of phosphorylation events, protein−protein interactions, and activation of signaling cascades ultimately leads to cell proliferation. These processes are tightly regulated; disruption of the signaling cascade at a number of points has been shown to result in loss of growth control as manifested in cellular transformation (reviewed in *6*, *7*).

The initial event in this whole process is ligand binding to the receptor. There have been numerous studies of EGF binding to the EGF receptor, and most studies have identified two classes of receptors, having low and high affinity (*8*−*11*). One hypothesis is that the low-affinity class represents ligand binding to a monomer, whereas the high-affinity class represents preformed dimers (*12*). While the EGF receptor can interact with other members of the EGF receptor family upon ligand binding, the presence of the two affinity classes is not dependent on the presence of other members of the receptor family (*13*−*15*).

Early morphological studies revealed that EGF binding results in receptor clustering and down-regulation (*16*−*20*). Cross-linking experiments have confirmed that binding of EGF induces the formation of receptor dimers (*21*−*24*). While it is generally thought that receptor dimerization leads to activation of the tyrosine kinase of the receptor, it is still unclear what role, if any, the observed higher-order receptor clustering plays in kinase regulation and subsequent signaling events. For this reason, additional experiments investigating the sizes of the oligomeric species present in the EGF/EGF receptor complex have been carried out with various spectroscopic probes attached to EGF. While cross-linking has the advantage that it can measure the state of oligomerization in the absence or presence of EGF, cross-linking can trap transient oligomers and thereby disrupt steady-state conditions. The use of a spectroscopic probe, in contrast, can potentially provide a direct physical method for measuring receptor oligomerization under steady-state or equilibrium conditions through quantitation of the effective sizes of the receptor complexes present, as reported by the rotational diffusion coefficients, which are inversely proportional to the correlation times for rotational diffusion of occupied receptors within the membrane.

A previous study carried out in our laboratories used spin-labeled EGF (SL-EGF) and saturation-transfer EPR (ST-EPR) to measure the rate of rotation of the occupied receptor in membrane vesicles (*25*). SL-EGF is a bifunctional adduct

† This work was supported by a grant from the National Institutes of Health (R01 GM55056).

* Correspondence should be addressed to either of these authors. J.V.S.: Department of Biological Sciences, Vanderbilt University, Box 351634, Station B, Nashville, TN 37235-1634, Phone: 615-322-4341, FAX: 615-343-6707, EMAIL: james.v.staros@vanderbilt.edu. A.H.B.: Department of Molecular Physiology and Biophysics, Vanderbilt University, Nashville, TN 37232-0615, Phone: 615-322-4235, FAX: 615-322-7236, EMAIL: al.beth@mcmail.vanderbilt.edu.

‡ Department of Biological Sciences.

§ Department of Molecular Physiology and Biophysics.

10.1021/bi015733q CCC: $22.00
Published on Web 01/18/2002

of bis(sulfo-*N*-succinimidyl)-[^{15}N,^{2}H$_{16}$]-doxyl-2-*spiro*-4′-pimelate (*26*) and [Lys3,Tyr22]-murine epidermal growth factor (*25*) in which the spin-label is bifunctionally linked through the amino terminus and the ϵ-amino nitrogen of Lys3 (*25*). The bifunctional attachment of the probe ensures that it is tightly coupled to the hormone and thus accurately reports the global rotational diffusion of the hormone (*25*). Istopic substitution of the protons in the spin-label with deuterons reduces inhomogeneous line broadening, increasing the signal-to-noise ratio and the spectral resolution, in particular in the ST-EPR time domain (*27*). Isotopic substitution of ^{15}N, which has two nuclear spin states, for ^{14}N, which has three nuclear spin states, simplifies the spectrum, and also increases the signal-to-noise ratio and the spectral resolution (*28*, *29*). The earlier EPR study (*25*) found that the occupied receptor had a rotational correlation time consistent with smaller oligomers, but was limited in three respects. One limitation was the presence of free SL-EGF, which necessitated the subtraction of the free signal from the total signal, leading to potential artifacts in the resultant ST-EPR spectrum. The second limitation was that an isotropic rotational model was used to analyze the motion of the SL-EGF/EGF receptor complex in the membrane. It is generally accepted that membrane proteins predominantly undergo uniaxial rotation, i.e., rotation about the membrane normal axis (*30*). Third, motional models containing multiple species were not considered, primarily due to the limited analytical methods available at the time. Methods for analyzing ST-EPR experiments in terms of a uniaxial rotational diffusion model have now been developed and applied to the study of the dynamic state of the anion exchange protein, band 3, in the human erthyrocyte membrane (*31*). More recently, methods for analyzing complex uniaxial rotational diffusion models including those with more than one component have been developed (*32*).

In the present study, we have prepared samples that contain very little unbound SL-EGF, obviating the need for spectral subtraction. The ST-EPR spectra from these samples were measured, and uniaxial rotational models were used to fit the data. We have found that the data are consistent with complex rotational mobility which may reflect two motionally distinct EGF/EGF receptor complexes in A431 membrane vesicles.

MATERIALS AND METHODS

Membrane vesicles from A431 cells were prepared using a modification (*33*) of the previously described method (*34*). SL-EGF, a bifunctional adduct of bis(sulfo-*N*-succinimidyl)-[^{15}N,^{2}H$_{16}$]-doxyl-2-*spiro*-4′-pimelate (*26*) and [Lys3,Tyr22]-murine epidermal growth factor (*25*), was made as previously described (*25*). All other reagents were at least reagent grade.

Sample Preparation. Samples for EPR were prepared as previously described (*25*) with slight modifications. After incubation of SL-EGF with the A431 vesicles, the samples were spun at 100000*g* in a tabletop ultracentrifuge (Beckman TLX, with TLA-100.4 rotor) for 10 min at 4 °C. The pellet was resuspended in 1 mL of 20 mM HEPES, pH 7.4, and centrifuged as above. The pellet was then resuspended in 20 mM HEPES to obtain a final volume of 300 μL. This sample was then transferred to a WG-813 quartz EPR flat cell (Wilmad Glass, Buena, NJ).

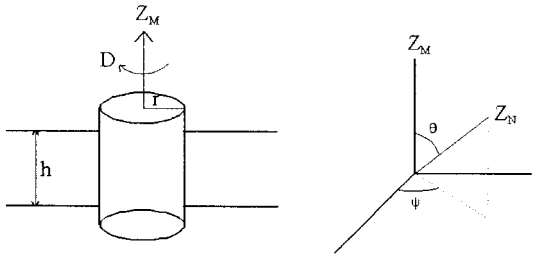

FIGURE 1: Uniaxial rotational diffusion model. The rate of rotation of a membrane protein is defined by the size of the transmembrane portion that lies within the highly viscous lipid bilayer. (Left panel) The transmembrane portion is described by a cylinder of radius *r* within the lipid bilayer of thickness *h*. The cylinder rotates about an axis that is perpendicular to the lipid bilayer, Z_M. The rate of motion is defined by the diffusion coefficient by the equation of Saffman and Delbruck (*30*). Rotational correlation times are inversely proportional to the diffusion constant. (Right panel) In EPR experiments, the shape of the spectrum is defined not only by the rate of rotation but also by the orientation of the spin-label, specifically the nitroxide moiety, relative to the axis of rotation. This orientation is described by the two angles θ and ψ.

Measurement and Analysis of EPR Spectra. Spectra were collected at X-band (9.8 GHz) with a Bruker EMX spectrometer equipped with an ER 4103 (TM_{110}) cavity. Temperature was maintained at 4 °C by blowing cooled N_2 gas through the front optical port of the cavity. The linear EPR spectrum was measured and analyzed to determine the principal elements of the nitroxide **A**- and **g**-tensors, as described (*35*). The ST-EPR spectra were obtained by using a 0.2 G microwave field, a 5 G Zeeman modulation field, and Zeeman modulation frequencies of 60, 80, and 100 kHz. Data were collected at multiple frequencies to increase the statistical significance of the fitting parameters. This increases the statistical significance by increasing the number of data points and minimizing the effect of any artifacts in any one single spectrum. The out-of-phase position for recording the second harmonic out-of-phase ST-EPR signal was determined by the self-null method (*36*). Analysis of ST-EPR spectra was carried out assuming a uniaxial rotational diffusion model and explicitly including Zeeman overmodulation effects (algorithm I) as previously described (*31*). The best-fit of the experimental data was determined on a statistical basis (minimum χ^2) as described (*35*). Error analysis was carried out by fixing one variable and allowing the remaining variables to minimize the fit to the data (*33*). The statistical significance between fits and error determination for individual parameters were done with an F-test (*33*). Simultaneous fitting of the three ST-EPR spectra yields 2600 degrees of freedom, leading to high statistical significance in the comparison of the different models. The parameters that describe uniaxial rotational motion are the diffusion coefficient for motion about the membrane normal axis and the two angles that describe the orientation of the spin-label relative to this axis (Figure 1).

RESULTS

EPR Experiments. Previous ST-EPR experiments investigating the rotational mobility of the SL-EGF/EGF receptor complex in A431 cell membranes were carried out at a single Zeeman-field modulation frequency of 50 kHz and fit with an isotropic rotational diffusion model (*25*). This model assumes that the protein is free to rotate about all axes, which

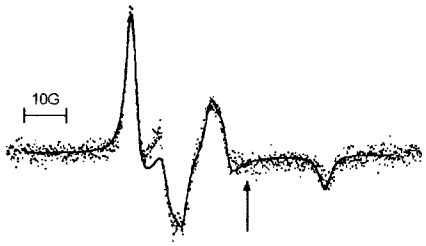

FIGURE 2: Linear EPR spectrum of SL-EGF bound to the EGF receptor. The arrow indicates the region of the spectrum where signal from free SL-EGF would appear. The lack of a signal is indicative of essentially no free SL-EGF present in the sample, obviating the need to carry out spectral subtraction to remove the signal that arises from free SL-EGF. The fit, assuming restricted mobility on the linear EPR time scale, yields **A**-tensors of 10.602, 10.579, and 46.593 G, and **g**-tensors of 2.008104, 2.005909, and 2.002487.

is not consistent with the restricted motion of a membrane protein. Since our previous EPR study, methods have been developed to analyze ST-EPR data obtained from membrane proteins in terms of the uniaxial rotational diffusion model (*31*) including models with more than one motional component (*32*). In addition, in the present study, spectra at multiple modulation frequencies were obtained and globally analyzed to more accurately describe the rotational mobility of the SL-EGF bound to the EGF receptor. Further, we have refined the method to produce SL-EGF bound to the EGF receptor in A431 membranes, yielding a preparation with essentially no free SL-EGF (Figure 2). This obviates the need to digitally subtract out the signal from unbound SL-EGF, thereby eliminating a potential source of error in the analysis. This spectrum was fit assuming that the spin-label is rigid on the linear EPR time scale to obtain the **A**- and **g**-tensors (Figure 2) to be used to fit the ST-EPR spectra. The values of the tensors obtained from this analysis are consistent with the rigid-limit assumption.

The ST-EPR spectra for SL-EGF bound to the EGF receptor were acquired at 60, 80, and 100 kHz (Figure 3). These three spectra were simultaneously fit using a single-component uniaxial model, yielding fit A (Figure 3, Table 1). The two main parameters that describe the motion in the uniaxial model are θ, the angle between the spin-label Z-axis and diffusion axis, and τ, the correlation time for uniaxial rotational diffusion, whereas ψ has little effect on the spectra at X-band microwave frequency (*31*). Error analysis was carried out by fixing one parameter at a given value and then letting the other parameters vary to minimize the difference between the fit and data (*33*). When the correlation time was held fixed at various values, no additional minima were found (Figure 4A). On the other hand, when the angle was varied, an additional minimum was found at $\theta \approx 29°$ that yielded a slightly lower χ^2 with a narrower minimum than the first minimum at $\theta \approx 90°$ (Figure 4B, Table 1).

The identification of two minima is an indication that there is not a single unique set of parameters for a one-component uniaxial rotational diffusion model that describe the data. This suggests that this model might not adequately describe the data and that there might be additional rotational motions occurring. In light of the presence of two receptor populations demarcated by their ligand-binding affinities (*14* and references cited therein), one possibility is that there are two receptor populations undergoing uniaxial rotational diffusion.

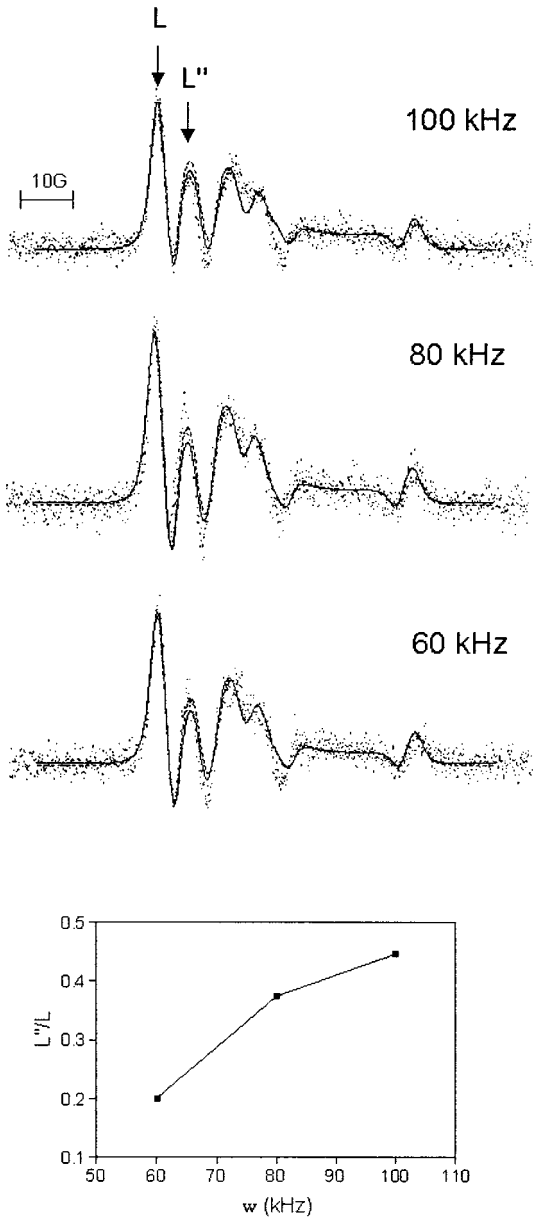

FIGURE 3: ST-EPR spectra of SL-EGF bound to the EGF receptor. Shown are the spectra collected at 60, 80, and 100 kHz (dots). Also shown are the two fits obtained, fit A (solid line) and fit B (dashed line). In Table 1 are the values of the parameters for the two fits. L and L″ indicate regions of the spectra sensitive to the changes in modulation frequency. Shown at the bottom of the figure is the ratio L″/L versus modulation frequency illustrating a change in the experimental spectra with changes in the modulation frequency. The region of the spectra where there is a difference between the two one-component fits corresponds to L″.

Table 1: One-Component Fits to the ST-EPR Spectra

	fit A	fit B
$\tau_{\|}$ (μs)	1.03	0.125
θ (deg)	90.3	28.6
ψ (deg)	−1.28	60.9
T_{1e} (μs)	5.5	4.9
T_{2e} (ns)	28	26
χ^2	1.80	1.77

The three ST-EPR spectra were then fit with a model with two independent populations undergoing uniaxial rotational diffusion (Figure 5, Table 2). It was found that the faster population comprised 55% (±20%), while the remaining

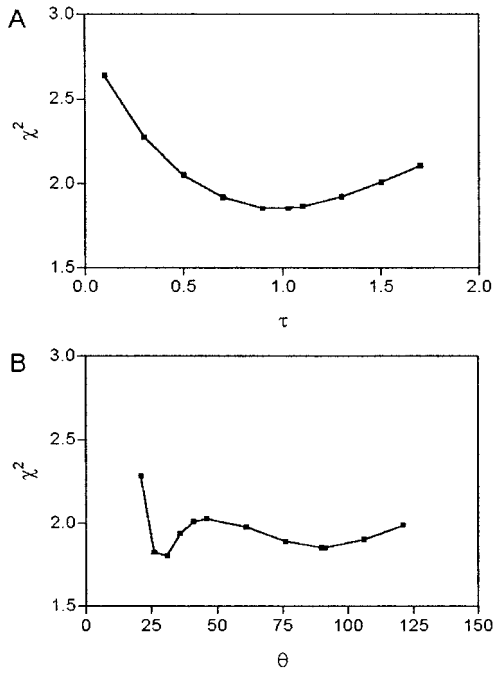

FIGURE 4: Confidence curves for the two parameters obtained from the initial fit of the ST-EPR spectra. (A) Shown are the χ^2 values for the fits at the fixed values of τ. The shallowness of the curve indicates the broad minimum that can be obtained from the starting values with $\theta \approx 90°$. (B) Shown are the χ^2 values for the fits at the fixed values of θ. Varying the angle allowed for the determination of a second minimum.

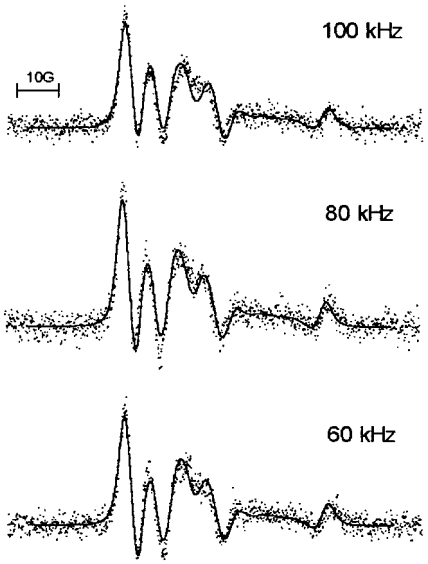

FIGURE 5: ST-EPR spectra of SL-EGF bound to the EGF receptor. Shown are the same spectra shown in Figure 3 (dots). Also shown is the fit for the two-component uniaxial model. In Table 2 are the values of parameters from this fit.

45% was undergoing slower rotational motion. This two-component model yielded a statistically better fit (95% confidence level) of the data compared with either of the one-component fits (Tables 1 and 2). The slow component is not as slow as the single component in fit A (Table 1), while the remaining values for the parameters of the two populations do not significantly differ from the two single-site fits obtained above: Compare fit A to component 1 and fit B to component 2 (Tables 1 and 2). While the addition of two similar spectra will yield a composite spectrum that is similar to its two constituent components, the improvement in the two-component fit does suggest that there are additional rotational motions occurring other than a single uniaxial rotating species.

Table 2: Two-Component Fit to the ST-EPR Spectra

	component 1	component 2
$\tau_{\|\|}$ (μs)	0.778	0.117
θ (deg)	89.5	28.5
ψ (deg)	−2.52	76.5
T_{1e} (μs)	3.8	4.7
T_{2e} (ns)	28	24
fraction	0.45	0.55
χ^2		1.65

DISCUSSION

Within the constraints of a model-dependent analysis, it is intriguing to correlate the two rotational populations of EGF/EGF receptor complexes identified in this study with previous reports of two populations of EGF receptors in A431 membrane vesicles identified by their differential ligand-binding properties, and termed high- and low-affinity populations (*33, 37*−*39*). It has previously been postulated that the low-affinity site is a monomer and the high-affinity site is a dimer (*12, 24, 40*). Based on the two rotational populations detected in this study, the faster species could represent the monomer, while the slower species could represent a dimer.

Previous studies have examined the binding of EGF modified with any of a variety of reporter groups (e.g., ^{125}I, biotin, or fluorescein) to the EGF receptor in A431 membrane preparations. Equilibrium binding experiments have consistently suggested two affinity classes of receptors, but have indicated a range of values for apparent affinity and for the relative proportions of the high- and low-affinity sites. For example, two studies carried out on A431 membranes have reported 25% (*33*) and 60% (*37*) for the percentage of high-affinity sites. Some of the variability in these two reports is likely to be attributable to differences in the conditions employed in the equilibrium binding assays, and perhaps to differences in the reagents themselves. While it is not practical to carry out detailed binding studies under the same conditions that were employed to collect the ST-EPR data (i.e., on densely packed membrane vesicles), it is interesting to note that the number of slow-rotating species determined in the current studies (45 ± 20%) falls within the range of values that have been reported for the percentage of high-affinity receptors in previous studies (*33, 37*). Studies on the kinetics of displacement of BSSDP-labeled wild-type EGF from EGF receptors solubilized from A431 membranes indicated two distinct off rates, of comparable amplitudes, that were suggestive of the presence of high- and low-affinity receptors (*41*). These latter studies suggest that the high- and low-affinity states of the receptor persist under a wide range of experimental conditions. The important point to be made with regard to the current work is that though it is speculative to correlate the slow rotating species with high-affinity receptors, this remains an intriguing possibility that is compatible with currently available binding data, and consistent with previously postulated models (*12, 24, 40*). Examination of this assignment in relation to previous measures of the oligomeric size of the EGF/EGF receptor

complex and to the expected size of a uniaxial rotating monomer, dimer, or larger oligomer is needed.

There have been previous examinations of the size of the EGF/EGF receptor complex using time-resolved phosphorescence anisotropy (TPA) of erythrosin-labeled EGF in the presence of the EGF receptor (*42*−*44*). The first set of experiments measured the time-resolved anisotropy of a saturating concentration of erythrosin-labeled EGF bound to A431 cells in suspension at various temperatures (*43*). These samples exhibited rising anisotropy curves with the rise time decreasing with increasing temperature, which was interpreted as indicating slower rotational mobility of the receptor at higher temperatures. It was concluded that the EGF/EGF receptor complex could form microclusters and that there was an increase in cluster size at higher temperatures (*43*), which was consistent with previous experiments on A431 cells that examined the extent of clustering of ferritin-EGF bound to the receptor, as followed by electron microscopy (*18*). The second study (*44*) was carried out on A431 membrane preparations made by the method of Thom et al. (*45*). These experiments, carried out similarly to the A431 cell experiments, also exhibited a rising anisotropy, which was interpreted to mean that EGF receptor rotated as a cluster with an increase in the cluster size at higher temperature (*44*). Further investigation of the difference in rotational mobility of high- and low-affinity receptors was studied by measuring the anisotropy of two concentrations of Er-EGF in the presence of A431 cells at 4 and 37 °C (*42*). At 4 °C, the high-affinity receptor population (low [Er-EGF]) displayed a smaller amplitude for the rise of the anisotropy as compared to the total receptor population, while at 37 °C, the difference was more pronounced, because the high-affinity receptors exhibited no microsecond rotational mobility. These results were interpreted to indicate that the state of receptor cluster formation was dependent on the affinity of the receptor (*42*).

The rotational dynamics of the EGF/EGF receptor complex have also been studied by ST-EPR (*25*). These experiments measured the rotational mobility of SL-EGF bound to EGF receptors in A431 membrane vesicles made by the method of Cohen et al. (*34*). The data from these experiments suggested that at 4 °C the spin-labeled EGF/EGF receptor complex had a rotational mobility consistent with that of a small oligomer such as a receptor dimer.

To gain a better understanding of the relationship between the previous time-resolved phosphorescence anisotropy and the previous and current ST-EPR results, the differences in the rates of rotational mobility of the two measurements can be examined. Both TPA and ST-EPR measure the rotational mobility in terms of a rotational correlation time, which is inversely proportional to the diffusion coefficient. For a membrane protein, the diffusion coefficient is given by (*30*)

$$D = \frac{kT}{4\pi\eta h r^2}$$

where k is Boltzmann's constant, T is temperature, η is the effective viscosity of the membrane at T, h is membrane bilayer thickness, and r is the radius of the transmembrane portion of the protein. The transmembrane portion of the EGF receptor is a single, presumably α-helical polypeptide segment that links the extracellular ligand-binding domain with the cytoplasmic kinase domain (*3*). When receptors dimerize, the transmembrane helices of the two receptor monomers are thought to interact (*46*, *47*). It has been shown that two parallel, interacting α-helices have a cross-sectional radius of approximately 10 Å (e.g., *48*). Assuming that the orientation of the two α-helices of an EGF receptor dimer is comparable, and using standard estimates for the effective bilayer viscosity of 2 P, a bilayer thickness of 40 Å, and a temperature of 4 °C leads to a predicted diffusion coefficient of approximately 4×10^5 s^{-1}. If the two α-helices in an EGF receptor dimer were not oriented parallel to each other, but were tilted relative to each other, the effective radius would increase with increasing tilt of the two helices. Examination by NMR of synthetic peptides corresponding to the transmembrane helices from the EGF receptor indicated that there is a 10−15° tilt between the two interacting transmembrane helices (*49*), which would not appreciably alter the 10 Å approximation used above.

In TPA, uniaxial motion of a membrane protein about the membrane normal will give rise to two correlation times that are related to the diffusion coefficient by 1/D and 1/4D (*50*, *51*). The previous TPA studies utilizing membranes (*44*) were able to detect only a single correlation time of approximately 20 μs. If the one correlation time is an average of the two components, 1/4D and 1/D (*43*), the diffusion coefficient would then be between 1.25×10^4 and 5.0×10^4 s^{-1}. Assuming a membrane viscosity of 2 P, this diffusion coefficient would correspond to a membrane protein with a radius between 30 and 60 Å which is larger than expected for an EGF receptor dimer, but consistent with a microcluster. On the time-scale of the TPA experiment, the submicrosecond rotational dynamics detected in the current study would not have been detected except for the effect on the apparent initial anisotropy value. In the ST-EPR measurements, the rotational correlation time is related to the diffusion coefficient by 1/6D. The initial ST-EPR studies fit the data to an effective isotropic rotational correlation time of 6 μs (*25*). This correlation time is an upper bound for the correlation time for uniaxial diffusion (see *51* for discussion of the relationship between "effective" correlation time from an isotropic model and the true correlation time for a generalized anisotropic model). In the present study, two populations have been identified, with correlation times of 0.12 and 0.78 μs, correlation times too fast to be detected in standard TPA measurements due to limitations in gating the photomultiplier tube following the excitation pulse and prompt fluorescence (*53*). Assuming a membrane viscosity of 2 P, the fast component would have a radius of approximately 5 Å, comparable to the size of a single transmembrane-spanning α-helix. The slower component would have a radius of approximately 13 Å, comparable to that expected for a transmembrane α-helix dimer.

Given these results, it is tempting to speculate that the two species correspond to receptor monomers and dimers, respectively. Due to uncertainties in the effective membrane viscosity and thickness, it is possible that the two rotational species are larger than discussed above. However, a change in size of each species would be inversely proportional to the square root of the change in either of the two parameters; therefore, the size of the two species should not be much larger than discussed above. An additional factor that would alter the estimate of the size of the species would be

nonparallel association of the transmembrane α-helices of the two receptors within a dimer. This effect should be negligible, since the effective radius of two transmembrane helices tilted 15° and interacting at one end of the helix would be on the order of 15 Å. Therefore, based on the correlation times determined in this study, the sizes of the two rotational species are not consistent with large oliogmers, but are consistent with monomers and dimers or somewhat larger oligomers, such as trimers or tetramers. Though there is ample evidence of higher order clustering of EGF receptors under some conditions (*18*, *44*, *54*), evidence presented in this study argues against a role for higher order receptor clustering in receptor activation, since the kinase of the EGF receptor under these conditions is stimulated by binding of SL-EGF (*25*).

The above discussion has focused on the rotational mobility of the two SL-EGF/EGF receptor complexes. In addition to the differences in mobility of the two populations, the orientation of the spin-label is also different (Table 2). The differences in the orientation could arise from two sources: (1) differences in orientation of the receptor-bound SL-EGF relative to the membrane normal axis or (2) differences in orientation of the spin-label relative to the EGF molecules to which it is covalently bound, which would translate into a difference in orientation relative to the membrane normal axis.

If the differences in orientation are due to differences in the orientation of EGF relative to the membrane normal, then this difference in orientation would suggest that the two EGF/EGF receptor species might be structurally or conformationally different, at least with regard to the orientation of the ligand-binding domain with respect to the membrane normal axis. This difference could be that EGF adopts a different conformation when binding to the two different receptor populations (Figure 6A), that EGF binds to the two different receptor populations in different orientations (Figure 6B), or that the two receptor populations have different orientations relative to the membrane while binding EGF in the same manner (Figure 6C). Any of the monomeric receptors in these models could represent the form that self-associates to form receptor dimers. The correspondence between the potentially different conformations and the different affinity states is unknown.

It is also possible that the differences in orientation between the two populations are not due to large conformational differences in the EGF/EGF receptor interaction. The potential difference in orientation of the spin-label relative to the membrane normal could arise from differences in the orientation of the spin-label relative to EGF. Upon conjugation of the spin-label to EGF, a chiral product is formed, with the two potential stereoisomers related by a 180° rotation of the doxyl ring. This symmetry in spin-label orientation should not alter the overall orientation of the spin-label relative to the membrane normal axis, since the analysis is not sensitive to the 180° symmetry of the spin-label. A second method of modification of the orientation of the spin-label relative to the EGF is that upon binding to the receptor there is an interaction of the spin-label with the receptor that alters its orientation relative to EGF and as a result its orientation relative to the membrane normal (Figure 6D). While the differences of spin-label orientation relative to the membrane normal might be dependent on the spin-label orientation relative to EGF, the differences in rotational mobility seen for the two populations are independent of the orientation of the spin-label relative to the membrane normal axis.

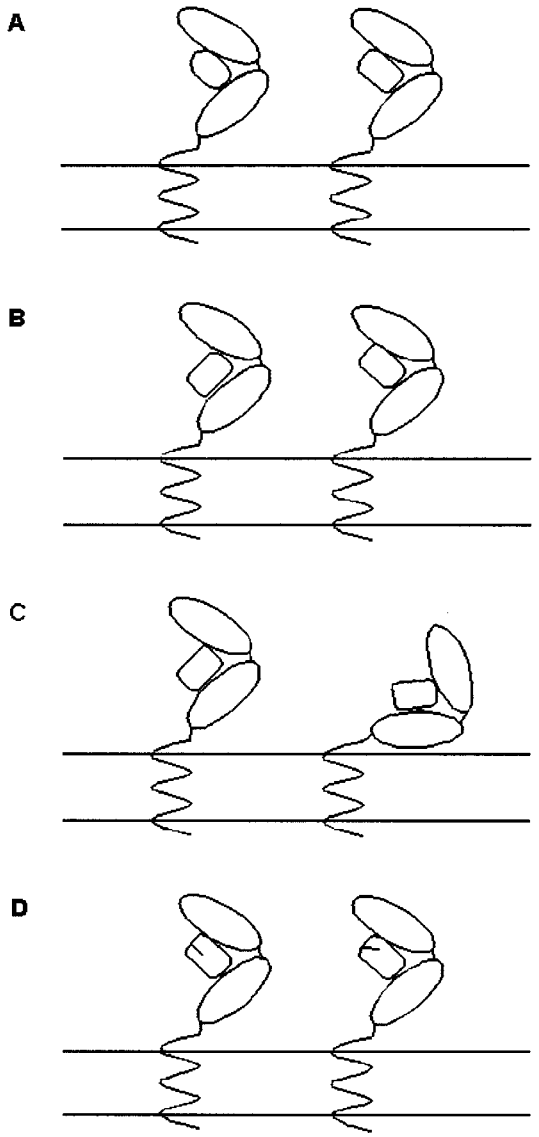

FIGURE 6: Models of EGF/EGF receptor orientations and binding. (A) Model showing the binding of EGF to the EGF receptor with two different conformations of the EGF. (B) Model showing a single orientation of the EGF receptor with EGF binding to the receptor in two different orientations. (C) Model showing EGF binding to the receptor in an identical manner, but with the receptor having a different orientation in the two states. (D) Model showing EGF binding the receptor in the same basic conformation with no large changes in orientation of the receptor. The line on EGF denotes the change in orientation between the two states of the amino-terminus as measured by the spin-label. Any of these monomeric receptors could represent the form that self-associates to form a receptor dimer.

Two considerations related to the global fitting of the ST-EPR data in Figure 5 and the conclusions drawn from these analyses merit discussion. First, the analyses have centered on uniaxial rotational diffusion being the dominant motional mode. Previous work has shown that intrinsic membrane proteins with multiple membrane-spanning segments such as band 3 (*31*, *32*) and bacteriorhodopsin (*55*) exhibit uniaxial rotational diffusion about the membrane normal axis as their major overall motional process. Much less work has been

devoted to characterizing rigorously the rotational diffusion of intrinsic membrane proteins such as the EGF receptor, where the majority of the protein is not embedded in the membrane, but rather exposed in globular domains outside the membrane. Clearly, the potential exists for some independent rotational motion of the extracellular ligand-binding domain relative to the single transmembrane α-helix of the receptor. The extent to which such motions would contribute to the ST-EPR signals would depend on both their amplitude and their frequency (*32*, *56*). The important point related to the current studies, however, is that a model based on the hindered uniaxial rotational diffusion of the transmembrane segment of the EGF receptor model results in excellent agreement with the experimental data obtained and in the recovery of rotational correlations times that are entirely consistent with uniaxial rotational diffusion dominating the rotational diffusion of the entire receptor complex. Second, it is clear that the two-component uniaxial model gives an excellent simultaneous fit of the three experimental spectra that were obtained at three different Zeeman modulation frequencies, and this fit is statistically better (95% confidence level) than any single-component uniaxial fit (Tables 1 and 2). While it would be possible to consider models with even more components, the high level of agreement between experiment and theory suggests that this would not result in substantial additional improvement over the two-component model. How these motions and orientations relate to ligand binding and differences in affinity, though, remains to be ascertained.

While it has been shown that the extracellular domain of the EGF receptor alone can form a homodimer upon EGF binding (*57*, *58*), the relationship of this interaction to high-affinity binding is uncertain, since it has been shown that both the transmembrane domain and the intracellular domain mediate high-affinity binding (*59*−*62*). This suggests that only direct structural experiments that can differentiate between the two different affinity states will be able to ascertain how the different EGF/EGF receptor orientations are related to differences in ligand affinities and any associated differences in receptor signaling. However, the current studies have provided data upon which one can formulate working hypotheses regarding the origin of high- and low-affinity receptor sites. For example, if dimerization leads to a structural rearrangement of the ligand-binding domain as suggested by the altered orientation of receptor-bound EGF relative to the membrane normal axis, then it is plausible that the structural rearrangement could alter the local structure of the EGF-binding pocket such that binding affinity is increased. This intriguing working hypothesis clearly warrants consideration in designing future experiments aimed at elucidating the molecular mechanism of multiple affinities for EGF binding to the EGF receptor.

CONCLUSION

Model-dependent analysis of ST-EPR spectra obtained at multiple frequencies of SL-EGF bound to the EGF receptor has detected complex rotational mobility, which is consistent with two uniaxial rotating species. Two such populations would be consistent with the two populations observed in ligand-binding studies and could correspond to the high- and low-affinity states. The faster rotating species has a rotational mobility consistent with a receptor monomer, while the slower rotating species has a rotational mobility consistent with a receptor dimer. In addition to the differences in rotational mobility, the orientation of the SL-EGF is different in the two populations. This suggests that the two populations of EGF/EGF receptor may not be conformationally equivalent. Further work is needed examining the potential structural differences between the two populations and how these differences might correspond to signaling from the EGF receptor complexes.

REFERENCES

1. Carpenter, G., King, L., Jr., and Cohen, S. (1978) *Nature 276*, 409−410.
2. Ushiro, H., and Cohen, S. (1980) *J. Biol. Chem. 255*, 8363−8365.
3. Ullrich, A., Coussens, L., Hayflick, J. S., Dull, T. J., Gray, A., Tam, A. W., Lee, J., Yarden, Y., Libermann, T. A., Schlessinger, J., et al. (1984) *Nature 309*, 418−425.
4. Buhrow, S. A., Cohen, S., and Staros, J. V. (1982) *J. Biol. Chem. 257*, 4019−4022.
5. Buhrow, S. A., Cohen, S., Garbers, D. L., and Staros, J. V. (1983) *J. Biol. Chem. 258*, 7824−7827.
6. Schlessinger, J. (2000) *Cell 103*, 211−225.
7. Wells, A. (1999) *Int. J. Biochem. Cell Biol. 31*, 637−643.
8. Baker, J. B., and Cunningham, D. D. (1978) *J. Supramol. Struct. 9*, 69−77.
9. Shoyab, M., De Larco, J. E., and Todaro, G. J. (1979) *Nature 279*, 387−391.
10. King, A. C., and Cuatrecasas, P. (1982) *J. Biol. Chem. 257*, 3053−3060.
11. Magun, B. E., Matrisian, L. M., and Bowden, G. T. (1980) *J. Biol. Chem. 255*, 6373−6381.
12. Ullrich, A., and Schlessinger, J. (1990) *Cell 61*, 203−212.
13. Fazioli, F., Minichiello, L., Matoska, V., Castagnino, P., Miki, T., Wong, W. T., and Di Fiore, P. P. (1993) *EMBO J. 12*, 3799−3808.
14. Stein, R. A., Wilkinson, J. C., Guyer, C. A., and Staros, J. V. (2001) *Biochemistry 40*, 6142−6154.
15. Wilkinson, J. C., Stein, R. A., Guyer, C. A., Beechem, J. M., and Staros, J. V. (2001) *Biochemistry 40*, 10230−10242.
16. Gorden, P., Carpentier, J. L., Cohen, S., and Orci, L. (1978) *Proc. Natl. Acad. Sci. U.S.A. 75*, 5025−5029.
17. Haigler, H., Ash, J. F., Singer, S. J., and Cohen, S. (1978) *Proc. Natl. Acad. Sci. U.S.A. 75*, 3317−3321.
18. Haigler, H. T., McKanna, J. A., and Cohen, S. (1979) *J. Cell Biol. 81*, 382−395.
19. McKanna, J. A., Haigler, H. T., and Cohen, S. (1979) *Proc. Natl. Acad. Sci. U.S.A. 76*, 5689−5693.
20. Schlessinger, J., Shechter, Y., Willingham, M. C., and Pastan, I. (1978) *Proc. Natl. Acad. Sci. U.S.A. 75*, 2659−2663.
21. Fanger, B. O., Austin, K. S., Earp, H. S., and Cidlowski, J. A. (1986) *Biochemistry 25*, 6414−6420.
22. Fanger, B. O., Stephens, J. E., and Staros, J. V. (1989) *FASEB J. 3*, 71−75.
23. Cochet, C., Kashles, O., Chambaz, E. M., Borrello, I., King, C. R., and Schlessinger, J. (1988) *J. Biol. Chem. 263*, 3290−3295.
24. Boni-Schnetzler, M., and Pilch, P. F. (1987) *Proc. Natl. Acad. Sci. U.S.A. 84*, 7832−7836.
25. Rousseau, D. L., Jr., Guyer, C. A., Beth, A. H., Papayannopoulos, I. A., Wang, B., Wu, R., Mroczkowski, B., and Staros, J. V. (1993) *Biochemistry 32*, 7893−7903.
26. Anjaneyulu, P. S., Beth, A. H., Sweetman, B. J., Faulkner, L. A., and Staros, J. V. (1988) *Biochemistry 27*, 6844−6851.
27. Beth, A. H., Perkins, R. C., Venkataramu, S. D., Pearson, D. E., Park, C. R., Park, J. H., and Dalton, L. R. (1980) *Chem. Phys. Lett. 69*, 24−28.
28. Beth, A. H., Balasubramanian, K., Wilder, R. T., Venkataramu, S. D., Robinson, B. H., Dalton, L. R., Pearson, D. E., and Park, J. H. (1981) *Proc. Natl. Acad. Sci. U.S.A. 78*, 4955−4959.

29. Beth, A. H., Venkataramu, S. D., Balasubramanian, K., Dalton, L. R., Robinson, B. H., Pearson, D. E., Park, C. R., and Park, J. H. (1981) *Proc. Natl. Acad. Sci. U.S.A. 78*, 967−971.
30. Saffman, P. G., and Delbruck, M. (1975) *Proc. Natl. Acad. Sci. U.S.A. 72*, 3111−3113.
31. Hustedt, E. J., and Beth, A. H. (1995) *Biophys. J. 69*, 1409−1423.
32. Hustedt, E. J., and Beth, A. H. (2001) *Biophys. J. 81*, 3156−3165.
33. Rousseau, D. L., Jr., Staros, J. V., and Beechem, J. M. (1995) *Biochemistry 34*, 14508−14518.
34. Cohen, S., Ushiro, H., Stoscheck, C., and Chinkers, M. (1982) *J. Biol. Chem. 257*, 1523−1531.
35. Hustedt, E. J., Cobb, C. E., Beth, A. H., and Beechem, J. M. (1993) *Biophys. J. 64*, 614−621.
36. Thomas, D. D., Dalton, L. R., and Hyde, J. S. (1976) *J. Chem. Phys. 65*, 3006−3024.
37. Gullick, W. J., Downward, D. J., Marsden, J. J., and Waterfield, M. D. (1984) *Anal. Biochem. 141*, 253−261.
38. Connolly, J. M., and Rose, D. P. (1987) *Cancer Lett. 37*, 241−249.
39. Carpenter, G., King, L., Jr., and Cohen, S. (1979) *J. Biol. Chem. 254*, 4884−4891.
40. Sorokin, A., Lemmon, M. A., Ullrich, A., and Schlessinger, J. (1994) *J. Biol. Chem. 269*, 9752−9759.
41. Faulkner-O'Brien, L. A., Beth, A. H., Papayannopoulos, I. A., Anjaneyulu, P. S., and Staros, J. V. (1991) *Biochemistry 30*, 8976−8985.
42. Zidovetzki, R., Johnson, D. A., Arndt-Jovin, D. J., and Jovin, T. M. (1991) *Biochemistry 30*, 6162−6166.
43. Zidovetzki, R., Yarden, Y., Schlessinger, J., and Jovin, T. M. (1981) *Proc. Natl. Acad. Sci. U.S.A. 78*, 6981−6985.
44. Zidovetzki, R., Yarden, Y., Schlessinger, J., and Jovin, T. M. (1986) *EMBO J. 5*, 247−250.
45. Thom, D., Powell, A. J., Lloyd, C. W., and Rees, D. A. (1977) *Biochem. J. 168*, 187−194.
46. Burke, C. L., and Stern, D. F. (1998) *Mol. Cell. Biol. 18*, 5371−5379.
47. Lofts, F. J., Hurst, H. C., Sternberg, M. J., and Gullick, W. J. (1993) *Oncogene 8*, 2813−2820.
48. Schertler, G. F., and Hargrave, P. A. (1995) *Proc. Natl. Acad. Sci. U.S.A. 92*, 11578−11582.
49. Jones, D. H., Barber, K. R., VanDerLoo, E. W., and Grant, C. W. (1998) *Biochemistry 37*, 16780−16787.
50. Rigler, R., and Ehrenberg, M. (1973) *Q. Rev. Biophys. 6*, 139−199.
51. Blackman, S. M., Cobb, C. E., Beth, A. H., and Piston, D. W. (1996) *Biophys. J. 71*, 194−208.
52. Beth, A. H., and Robinson, B. H. (1990) in *Biological Application of Spin Labeling* (Berliner, L. J., and Reuben, J., Eds.) pp 179−253, Academic Press, New York.
53. Yoshida, T., Jovin, T., and Barisas, B. (1989) *Rev. Sci. Instrum. 60*, 2924−2928.
54. St-Pierre, P. R., and Petersen, N. O. (1992) *Biochemistry 31*, 2459−2463.
55. Cherry, R. J., and Godfrey, R. E. (1981) *Biophys. J. 36*, 257−276.
56. Howard, E. C., Lindahl, K. M., Polnaszek, C. F., and Thomas, D. D. (1993) *Biophys. J. 64*, 581−593.
57. Lemmon, M. A., Bu, Z., Ladbury, J. E., Zhou, M., Pinchasi, D., Lax, I., Engelman, D. M., and Schlessinger, J. (1997) *EMBO J. 16*, 281−294.
58. Ferguson, K. M., Darling, P. J., Mohan, M. J., Macatee, T. L., and Lemmon, M. A. (2000) *EMBO J. 19*, 4632−4643.
59. Schaefer, G., Akita, R. W., and Sliwkowski, M. X. (1999) *J. Biol. Chem. 274*, 859−866.
60. Tanner, K. G., and Kyte, J. (1999) *J. Biol. Chem. 274*, 35985−35990.
61. Van der Heyden, M. A., Nievers, M., Verkleij, A. J., Boonstra, J., and Van Bergen en Henegouwen, P. M. (1997) *FEBS Lett. 410*, 265−268.
62. Worthylake, R., and Wiley, H. S. (1997) *J. Biol. Chem. 272*, 8594−8601.

BI015733Q